Synthesis, Structural and Optical Characterization of Uncalcined Lanthanum Oxide Nanoparticles by Co-Precipitation Method

[1*]N.Ramjeyanthi, [2,3]M.Alagar,[1]D.Muthuraman

[1*]Department of Physics, PSN College of Engineering & Technology, Tirunelveli-627152, Tamil Nadu, India

[2]Centre for Research and Post Graduate studies in Physics, AyyanadarJanakiammal College, Sivakasi-626123,Tamil Nadu, India

[3]Department of PG Physics,MannarThirumalaiNaicker College, Madurai-625004, Tamil Nadu, India

*Email: jeyanthirams@gmail.com

Abstract: In this work, Lanthanum oxide (La_2O_3) nanoparticles were synthesized by co-precipitation method and analyze their structural and optical properties. X-ray diffraction (XRD) pattern confirms the formation of hexagonal structured La_2O_3 nanoparticles with slight mixed state of hydroxides and carbonates. The crystallite size of La_2O_3 nanoparticles was obtained by using Debye-Scherer's calculation and Williamson-Hall (W-H) plot analysis methods. The existence of La-O stretching band at < 800 cm^{-1} in the Fourier transformed infrared (FTIR) spectrum confirms the formation of La_2O_3 nanoparticles. Scanning electron microscopy (SEM) images represents the appearance of spherical shaped particles with nanosize regime. Further, the optical properties of La_2O_3 nanoparticles were investigated from UV-visible diffuse reflectance spectroscopy and the indirect band gap value was found to be 5.35 eV. Photoluminescence (PL) spectrum exhibits the broad emission peak in the wavelength ranges of 356-732 nm under the excitation of 230 nm.

Keywords: La_2O_3, uncalcined, Nanoparticles, co-precipitation, crystallite size, optical properties.

1. INTRODUCTION

In recent years Rare earth oxides (REO) have increasing the demand due to their excellent structural stability at high temperature, active surface sites, chemical and optical properties with greatly influenced luminescence efficiency in the visible domain [1,2]. The outstanding luminescence characteristics of the materials has increasing their applications in the field of technology, industry and environmental. The high influenced luminescence behaviour of rare earth oxides are mainly initiated from the partially filled 4f electronic shell in their structures [3]. There are many factors can affect the bandgap and luminescence properties of the materials such as preparation methods, host materials initial purity, thermal treatments and size of the particles. Compared to microstructure of these rare earth oxides, the nanostructure can exhibits enhance luminescence properties.so the size controlled synthesis methods are more important to obtain better luminescence properties in the rare earth materials [4].

Amongst rare earth oxides, lanthanum oxide (La_2O_3) has potentially more useful materials for their wide range of optical and electronic applications due to their large energy band gap lies $E_g > 4$ eV and which is also contains lowest lattice energy with high dielectric constants of $\varepsilon = 27$ pF/m [5,6]. It is also important component in catalyst of automobile exhauster [7], high k gate dielectric materials [8], optical filters [9], strengthening agent in structural material [10], magnetic data storage devices [11], biosensor and water treatment applications [12]. In water treatment applications La_2O_3 nanoparticles provide enhanced photocatalytic activities which may causes by the presence of many active sites for free

radicals scavenging because of their large surface to volume ratio and their mixed valence states for unique redox properties [13]. Moreover, the crystallites with nanosize regime can be easy to confine the movement of phonons in La_2O_3 nanoparticles.

In the earlier works, La_2O_3 nanoparticles were synthesized by using several synthesis techniques such as sol-gel [14], spray deposition [15], solvothermal [16], hydrothermal [17] and combustion [18] methods. Among all these methods, a co-precipitation method offers many advantages include the simple process, low cost, high crystallization degree, pure phase and particle size of powders are controllable [19]. In this advantages, La_2O_3 nanoparticles were prepared from the co-precipitation method by using the lanthanum nitrate hexahydrate $(La(NO_3)_3.6H_2O)$ as a precursor and sodium hydroxide (NaOH) can act as a precipitating agent. Furthermore, the physical, chemical, morphological and optical characteristics of obtained La_2O_3 nanoparticles were characterized by using the XRD, SEM, FTIR, UV-Visible DRS and PL analytical tools respectively.

2. EXPERIMENTAL DETAILS

2.1 Materials:

Lanthanum (III) nitrate hexahydrate $(La(NO_3)_3.6H_2O$ (433.007 g/mole; 99.9% purity) and Sodium hydroxide (NaOH) (40.00 g/mole; 99.9% purity) were purchased from Himedia Laboratories Pvt.Ltd. The above chemicals were used without any further purification. In addition, Distilled water and ethanol were used for solvent and washing process.

2.2 Synthesis of La_2O_3 nanoparticles:

0.1M of Lanthanum nitrate haxahydrate was dissolved in distilled water with constant stirring for 30 minutes at room temperature. Further, 0.3M of aqueous NaOH solution was added to the Lanthanum nitrate solutions by drop-wise at room temperature with constant stirrer and allows to the settle down of solution. The non-reacted nitrate present in the resultant precursor solution was completely removed through washing process with the assist of water and ethanol in several times. After completion of washing process, the appearance of the final precursor solution was changes their colour from dark blackish into whitish colour. The final product was filtered and dried at room temperature for 96 hours. At last, obtained powder samples were grained by using mortar and pestle and obtain the ultrafine La_2O_3 nanoparticles.

3. RESULTS AND DISCUSSION

3.1 Structural Analysis:

The crystallinity and phase purity of the uncalcinedLa_2O_3 nanoparticles was characterized by using X-ray diffraction (XRD) in the diffraction angle (2θ) ranges between 10° to 80° with scanning rate of 5° per minute. The XRD pattern of uncalcinedLa_2O_3 nanoparticles contains several peaks as shown in Fig. 1(a). The obtained XRD characteristics peaks shows that the maximum intensity peak was observed at (002) and other extended peak intensity were observed at (001), (100), (101), (411), (012), (103), (110), (111) and (200) crystal planes. The well extended intensity peaks are indicates the polycrystalline nature and size reduction of La_2O_3 nanoparticles. other than extended intensity peaks a very weak intensity peaks also observed in the XRD pattern which may arises due to the presence of hydroxide and carbonate states in uncalcined La_2O_3 nanoparticles. All the identified La_2O_3 peaks are good agreement with the JCPDS file (50-0602) and well reliable with earlier reports [20,21]. It clearly indicates the formation of hexagonal structured of La_2O_3 nanoparticles with slight mixed state of lanthanum hydroxide and carbonates. So further calcinations are essentials to remove the hydroxide and carbonate phases to obtain pure form of La_2O_3.

The average crystallite size (D in nm) of the La_2O_3 nanoparticles was found by using the Debye-Scherrer formula [22] as follows,

$$D = \frac{K\lambda}{\beta cos\theta} \tag{1}$$

Where K is a constant (0.89), λ is the wavelength of X-ray $(\lambda=1.5418A^0)$, θ is the diffraction angle for the peak and β is full width at half maximum (FWHM). Taking in to the account of instrumental broadening, average crystallite size of La_2O_3 nanoparticles also calculated by using Williamson-Hall plot analysis [23]. The equation used for Hall plot analysis is,

$$\beta cos\theta = \frac{0.9\lambda}{D} + 4\varepsilon sin\theta \tag{2}$$

Where, β is the FWHM, ϵ is the lattice strain and D is the crystallite size of the samples. The plot is drawn between $4\sin\theta$ vs $\beta\cos\theta$ as shown in Figure 1(b). The linear fit equation data from the W-H plot was used to calculate the crystallite size (using intercepts value) and micro strain (slope) of the particles. The estimated crystallite size of La_2O_3 nanoparticles from W-H plot analysis are tabulated and compared to the DS results as shown in table 1.The crystallite size observed from the W-H method is slightly high compared to the size measured from the Debye-Scherrer method. It may ascribed to be removal of broadening error was achieved in the W-H plot. In addition to the crystallographic parameters like microstrain and dislocation density (δ) of the La_2O_3 nanoparticles were calculated from the XRD data by using the following equations [24],

$$\delta = \frac{1}{D^2} \tag{3}$$

$$\epsilon = \frac{\beta\cos\theta}{4} \tag{4}$$

The calculated crystal parameters were summarized and tabulated. The crystalline parameters are also confirmed the formation of hexagonal structure of La_2O_3.
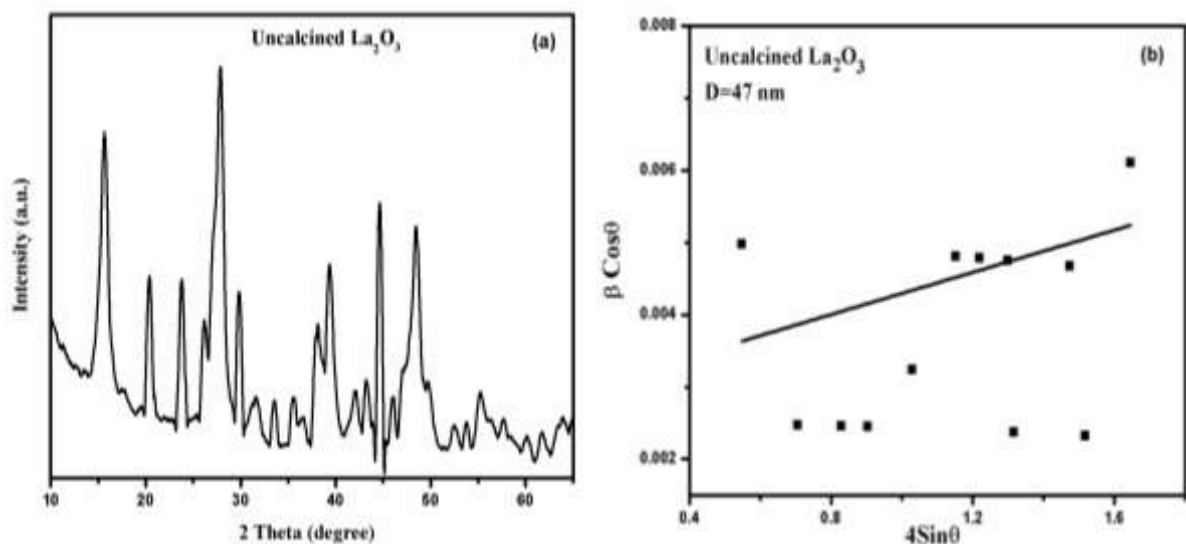
Figure 1: (a) XRD Pattern (b) W-H Plot of the uncalcined La_2O_3 nanoparticles

Table 1: The different crystal lattice parameters of uncalcined La_2O_3 nanoparticles

Sample	Dislocation density (δ) x10^{14} nm^{-2}	Microstrain (ϵ) x 10^{-3}		Average crystallite size (nm)	
		W-H plot	Theoretical	Debye-Scherrer	W-H plot
La_2O_3	4.5	1.563	2.031	41	47

3.2 Morphology Analysis:

Scanning electron microscope (SEM) is the powerful magnification tool to detect the grain size, shape and surface morphology of nanoparticles. The obtained SEM micrographs of the synthesized La_2O_3 nanoparticles were shown in Figure 2. It clearly shows that the surface of uncalcined La_2O_3 nanoparticles is spherical in shape with uniform size distribution. Apart from this some particle agglomerations was also observed in the SEM images. The obtained morphology was good agreement with Literature [25, 26]. Due to the presence of particle agglomerations, an exact value of particle size was not easy to calculate. An approximate value of average particle size was found to be 37 nm by using the ImageJ software.
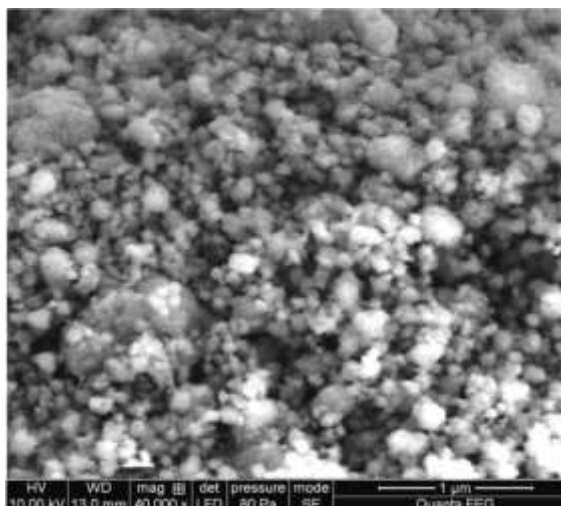
Figure 2: SEM image of the uncalcinedLa$_2$O$_3$ nanoparticles

3.3 FTIR Spectra Analysis:

The existence of metal-oxygen bonding and other functional groups of uncalcinedLa$_2$O$_3$ nanoparticles were analyzed by using FTIR spectroscopy. Figure 3.shows that, the FTIR spectra of uncalcined La$_2$O$_3$ nanoparticles captured in the wave number range of 400 to 4000 cm^{-1}. The obtained bands were well correlated with the literature [27, 28]. A weak absorption band at 3606, 3440 and 3144 cm^{-1} are assigned by the water and hydroxyl stretches (O-H stretching). Similarly, a very weak bond appeared at 1502 cm^{-1} due toOH bending vibrations of water molecules. The bands observed at 2929 and 2849 cm^{-1} are arises with respect to C-H bonding. The band at 2378, 1437 and 1115 cm^{-1} may appear from the absorption of atmospheric CO$_2$. The absorption band at 865, 727 and 635 cm^{-1} represent the metal-oxygen Stretching (La-O stretch) which confirm the formation of La$_2$O$_3$ nanoparticles.
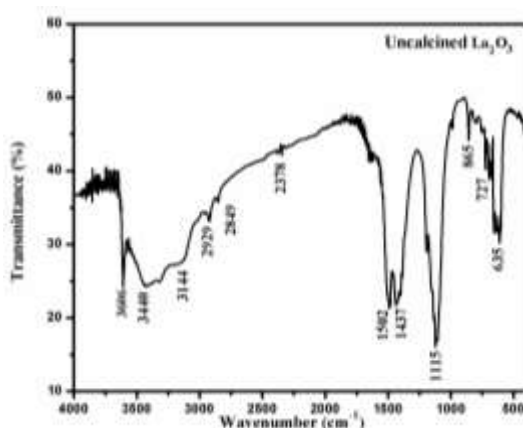
Figure 3: FTIR Spectra of uncalcinedLa$_2$O$_3$ nanoparticles

3.4 UV-Visible DRS Spectra Analysis:

The optical properties of the uncalcined La$_2$O$_3$ nanoparticles was analysed by using UV visible diffuse reflectance spectroscopy. The Figure 4(a) shows that, the obtained reflectance spectra of La$_2$O$_3$ nanoparticles in the wavelength range of 200-900 nm. The data collected from the refection spectra, the indirect band gap value of La$_2$O$_3$ nanoparticles was calculated by using Kubelka-Munk (K-M method) equation [29, 30] as follows,

$(h\upsilon F(R))^{1/2} = A(h\upsilon - E_g)$

Where $F(R) = (1-R)^{1/2}/2R$, h is a Planks constant, υ isthelight frequency, A is the absorption coefficient and E$_g$ is the band gap energy.

The K-M plot was drawn between $(h\upsilon F(R))^{1/2}$vshυ as shown in Figure 4(b). A straight line is drawn tangent to the point of interaction with hυaxis whichgivesthe indirect energy band gap value of 5.35 eV. The obtained E_g value demonstrate that red shift occur on the nanoparticles. The attained band gap value was good agreement with literature [31].
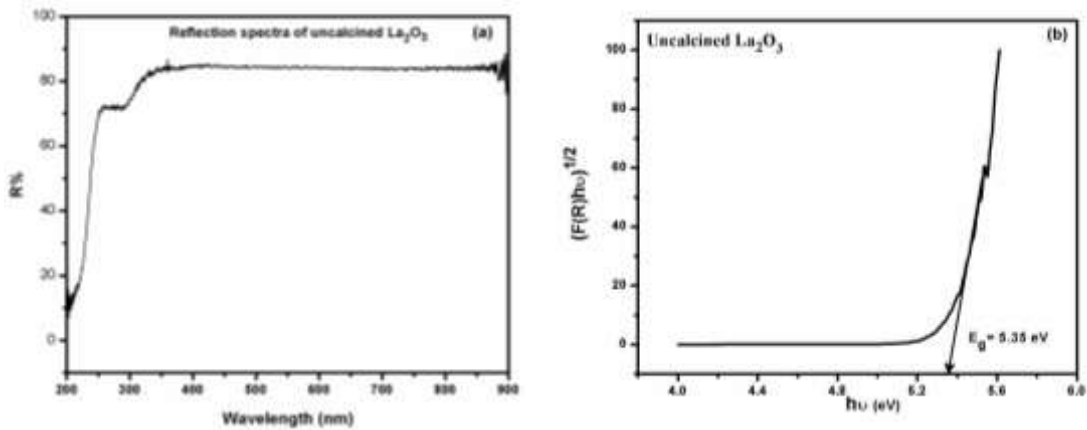
Figure 4: (a) Room temperature optical reflectance spectra and (b) K-M Plot of La$_2$O$_3$ nanoparticles

3.5PL spectra Analysis:

The electronic structure, transfer behaviour of electron-hole pair in semiconducting materials has been widely investigated by using Photoluminescence (PL) spectroscopy. Compared to other optical characterization tools PL is the more leading technique to find optical properties of the material without destructing the sample. The examined PL spectra of uncalcinedLa$_2$O$_3$ nanoparticles in the wavelength range of 300-800 nm was recorded under the excitation wavelength of 230 nm as shown in Figure 5.

The PL spectrum of uncalcined La$_2$O$_3$ nanoparticles exhibits a sharp and strong intensity peaks which may attributed to the quicker recombination of excited electrons with valence band holes. Further, the weak and low intensity peaks ascribed by the lower recombination process. The obtained PL spectra shows that, a peaks at 356, 365, 450, 462, 483, 492, 698 and 732 nm respectively. The peak at 356 and 365 nm appeared in the UV region which attributed to the UV band edge emission. Apart from that, four visible emission peaks were observed 450, 462, 483 and 492 nm in the blue region which are assigned by the phenomenon of defects, oxygen vacancies in the interstitials sites of La$_2$O$_3$ nanoparticles. The high intensity red emission peak at 698 nm and weak emission peak at 732 nm was ascribed by the radiativerelaxational transition phenomenon of La^{3+} ions facilated by the surface defects. The obtained results were concord with the earlier reports [32,33]
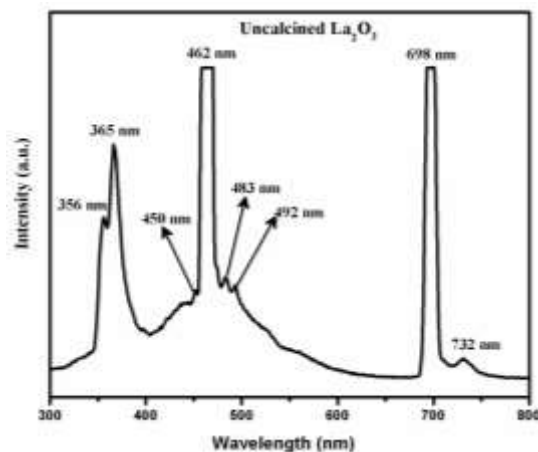
Figure 5: Room temperature photoluminescence (PL) Spectra of uncalcined La$_2$O$_3$nanoparticles

4. CONCLUSIONS

 Lanthanum oxide (La_2O_3)nanoparticles were successfully synthesized by co-precipitation method at room temperature. The hexagonal structured La_2O_3 nanoparticles with slight mixed state of lanthanum hydroxide and carbonates were confirmed from XRD pattern and crystallite size of the particles is found to be 41 nm (Scherrer method) and 47 nm (W-H Plot). The XRD results suggested that, the further calcinations is required to remove the hydroxides and carbonates and then obtain pure phase of La_2O_3 nanoparticles. The SEM image of La_2O_3 nanoparticles shows thatthe particles are spherical in shape with some agglomerations. FTIR results were confirmed the presence of La_2O_3 from the metal-oxygen stretching band at 865, 727 and 635 cm^{-1}. The high energy indirect band gap of 5.35 eV was obtained from KM plot using DRS reflection spectra, which indicate the La_2O_3 have good optical response. The PL spectrum indicates the La_2O_3 nanoparticles having violet-blue-red emissions and the results also confirm the reduction in the recombination rate of electron-hole pairs due to the oxygen vacancies.

REFERENCES

[1]   G.Adachi, N.Imanka, Z.C.Kang, Binary Rare Earth Oxides, Kluwer Academic Publishers, Newyork**(2004).**

[2]   Adrian Kitai, Luminescent material and application,JohnWiley & Sons Ltd,Canada (2008).

[3]   M Mogensen, N M Sammes and G A Tompsatt 2000 Soild State Ion 129, **63**.

[4]   Junwei Zhao, TiekunJia, Xiaofeng Wang and Xianggui Kong, controlled synthesis of water-soluble $NaYF_4$:Yb^{3+}, Er^{3+} nanoparticles with surfactant dependent properties, "Journal of nanomaterials", 2014, (2014), **1-7.**

[5]   Zhang, Ning, Ran Yi, Libin Zhou, GuanhuaGao, Rongrong Shi, GuanzhouQiu and Xiaohe Liu, "Lanthanide hydroxide nanorods and their thermal decomposition to lanthanide oxide nanorods", Material Chemistry and Physics 114, no.1 (2009), **160-167.**

[6]   Bedoya, Cedric, guiglielmo G, Condorelli, Sebastiana T. Finocchiaro, Alessandro Di Mauro, Dario Atanasio, I.L. Fragala, Lorena Cattaneo and Sergio carella, "MOCVD of lanthanum oxides from La (tmhd) 3 and La (tmod) 3 precursors: A thermal and kinetic investigation", Chemical vapor deposition 12, no.1 (2006), **46-53.**

[7]   Gamal A.H. Mekhemer, Basma A.A. Balboul, "Colloids Surf., A Physicochem. Eng. Asp." 181, (2001), **19–29**.

[8]   P. Pisecny, K. Husekova, "Mater. Sci. Semicond. Proces," 7 , (2004), **231-236**.

[9]   S. Wang, W. Wang, Y. Qian, "Thin Solid Films" ,372, (2000), **50–53.**

[10]   J.C. Yang, Z.R. Nie, Y.M. Wang, "Appl. Surf. Sci." 215, (2003), **87–95.**

[11]   NejadS J, Abolghasemi H, Moosavian M A, Golzary A, Maragheh M G. Fractional factorial design for the optimization of hydrothermal synthesis of lanthanum oxide nanoparticles under supercritical water condition, "J. Supercrit. Fluids", 52, (2010), **292.**

[12]   Khanjani S, Morsali A. Synthesis and characterization of lanthanum oxide nanoparticles from thermolysis nanostructured supramolecular compound, "J. Mol. Liq", 153, (2010),**129**.

[13]   Y Wang , T Mori, Li J and T Ikegami, "J.Am.Ceram.Soc", 3105.4, (2002), **85**

[14]   M Alifanti , B Baps & N Blangenois, 'Chemical material", 15 (2003) **395**.

[15]   Hamid Reza Ghaffarain, MahboobehSaiedi, Mohammad Ali Sayyadnejad, AlimoradRashidi, Synthesis of ZnO Nanoparticles by Spray Pyrolysis Method, "Iranian Journal of Chemistry & Chemical Engineering – International English Edition", 30(1), (2011), **1-6.**

[16]   Jianlin Li, Qingliu Wu and Ji Wu, Synthesis of Nanoparticles via Solvothermal and Hydrothermal method, "Handbook of nanomaterials", (2015), **1-28.**

[17]   S Phoka, S Pinisoontorn, P Chirawatkul, Y Poo-arporn& S Maensir, "Nanoscale Research letters", 7 (2012) **425**.

[18]   S Bojana, A Zeljka, A Nadica, K Radenka, MiogragMitric, M Ametia& DD Miroslav, "ActaChimSlov", 55, (2008), **486**.

[19] Jing Luo, Juan Chen, Wenzhao Li, Zhiliang Huang , Changlian Chen, "MATEC Web of Conferences" 26, (2015), **01007.**

[20] V.G.Shinde, V.B.Gaikwad, M.K.Deore, Synthesis of Lanthanum Oxide (La_2O_3)Nanoparticles by Hydrothermal method and studies it's Physical Properties, "International Journal of Chemical and Physical Sciences", 7, (2018), **669-674.**

[21] S.Karthikeyan, A.Dhayal Raj, A.AlbertIrudayaraj, D.MagimaiAntoniraj, Effect of temperature on the properties of La_2O_3 nanostructures, "Science Direct", 2 ,(2015), **1021-1025**.

[22] Hung-Yi Chang, Huey-Ing Chen, "J.Crystal Growth" 283, (2005), **457**.

[23] G.K.Williamson, W.Hall, "ActaMetallurgica", 1, (1953), **22**

[24] R. Suresh, V. Ponnuswamy, R. Mariappan. "Appl. Surface Science' 273, (2013), **457-464.**

[25] AmanullakhanA.Pathan, Kavita R .Desai and C.P.Bhasin, Synthesis of La_2O_3 Nanoparticles Nanoparticles using Glutaric acid and Propylene glycol for Future CMOS Applications, "International Journal of Nanomaterials and Chemistry", 3 (2), (2017), **21-25.**

[26] BrabuBalusamy, Yamuna GowriKandhasamy, AnithaSenthamizhan, GopalakrishnanChandrasekaran, Characterisation and bacterial toxity of lanthanum oxide bulk and nanoparticles, "Journal of Rare Earths" 30 (12), (2012), **1298.**

[27] S.Karthieyan&M.Selvapandiyan, Effect of Annealing Temperature on the Properties of Lanthanum Oxide (La_2O_3) Nanoplates by Reflux Routes, "International Journal of Engineering Sciences &Research", 7(3), (2018), **559-562.**

[28] Tsoutsou.D, G.Scarel, A.Debernardi, S.C.Capelli, S.N.Volkos, L.Lamagna, S.Schamm, P.E.Coulon and M.Fanciulli, Infrared Spectroscopy and X-ray diffraction studies on the crystallographic evolution of La_2O_3 films upon annealing", "Microelectronic Engineering", 85(12), (2008), **2411-2413.**

[29] P Kubelka, F Munk "Z Tech phys" 12, (1931), **593**.

[30] P Kubelka "J Opt Am" 38, (1948), **448**

[31] S.Karthieyan&M.Selvapandiyan, Synthesis of Nanocrystalline Lanthanum Oxides La_2O_3 Powder at Reflux routes, "International Journal of Computer Science and Communication Networks", 7(3), (2017), **70-78.**

[32] Cheguo Hu, Hong Liu, Wenting Dong, Yiyi Zhang Bao, Changshi Lao and ZhongL.Wang, La(OH)3 and La2O3 Nanobelts- Synthesis and Physical Properties, "Adv.Mater", 10, (2007), **470-474.**

[33] J.Y.Li,Luminescent Materials of Rare Earths and Their Applications, "Chemical Industry, Beijing", (2003), **8.**